Self-Consistent Ornstein-Zernike Approximation (SCOZA) and exact second virial coefficients and their relationship with critical temperature for colloidal or protein suspensions with short-ranged attractive interactions

Domenico Gazzillo and Davide Pini

Citation: The Journal of Chemical Physics **139**, 164501 (2013); doi: 10.1063/1.4825174
View online: http://dx.doi.org/10.1063/1.4825174
View Table of Contents: http://scitation.aip.org/content/aip/journal/jcp/139/16?ver=pdfcov
Published by the AIP Publishing

Self-Consistent Ornstein-Zernike Approximation (SCOZA) and exact second virial coefficients and their relationship with critical temperature for colloidal or protein suspensions with short-ranged attractive interactions

Domenico Gazzillo[1,a)] and Davide Pini[2,b)]
[1]*Dipartimento di Scienze Molecolari e Nanosistemi, Università di Venezia, S. Marta DD 2137, I-30123 Venezia, Italy*
[2]*Dipartimento di Fisica, Università di Milano, via Celoria 16, I-20133 Milano, Italy*

(Received 30 July 2013; accepted 30 September 2013; published online 22 October 2013)

We focus on the second virial coefficient B_2 of fluids with molecules interacting through hard-sphere potentials plus *very short-ranged* attractions, namely, with a range of attraction smaller than half hard-sphere diameter. This kind of interactions is found in colloidal or protein suspensions, while the interest in B_2 stems from the relation between this quantity and some other properties of these fluid systems. Since the SCOZA (Self-Consistent Ornstein-Zernike Approximation) integral equation is known to yield accurate thermodynamic and structural predictions even near phase transitions and in the critical region, we investigate B_2^{SCOZA} and compare it with B_2^{exact}, for some typical potential models. The aim of the paper is however twofold. First, by expanding in powers of density the condition of thermodynamic consistency included in the SCOZA integral equation, a general *analytic* expression for B_2^{SCOZA} is derived. For a given potential model, a comparison between B_2^{SCOZA} and B_2^{exact} may help to estimate the regimes where the SCOZA closure is reliable. Second, following the Vliegenthart-Lekkerkerker (VL) and Noro-Frenkel suggestions, the relationship between the critical B_2 and the critical temperature T_c is discussed in detail for two prototype models: the square-well (SW) potential and the hard-sphere attractive Yukawa (HSY) one. The known simulation data for the SW model are revisited, while for the HSY model new SCOZA results have been generated. Although B_2^{HSY} at the critical temperature is found to be a slowly varying function of the range of Yukawa attraction Δ_Y over a wide interval of Δ_Y, it turns out to diverge as Δ_Y vanishes. For fluids with very short-ranged attractions, such a behavior contrasts with the VL assumption that B_2 at the critical temperature should be nearly independent of the range of attraction. A very simple analytic representation is found for the available Monte Carlo data for T_c^{HSY} and B_2^{HSY} as functions of the range of attraction, for Δ_Y smaller than half hard-sphere diameter. © *2013 AIP Publishing LLC*. [http://dx.doi.org/10.1063/1.4825174]

I. INTRODUCTION

About fifty years ago computer simulations established that liquids cannot exist in the absence of *attractive* interactions.[1–3] More recently, it was ascertained that even the *range of attraction* is essential, since it can affect the phase behavior of a substance. In fact, when the attraction range falls below a critical value, a liquid phase cannot be stable, and the gas-liquid or liquid-liquid phase transitions become metastable with respect to freezing.[4]

In colloidal or protein suspensions, it is most common to encounter both attractive and repulsive interactions having very short ranges, in comparison to the size of the macromolecules. In particular, in solutions of globular proteins, the short-range character of the attractions seems to be the cause of metastability for a liquid-liquid phase separation occurring below the fluid-solid transition.[5] Furthermore, the presence of such a metastable transition cannot be neglected, since it has some noticeable effects on the crystallization behavior of these proteins.[6]

Fluids with very short-ranged attractions represent a true challenge for the liquid state theory. In fact, all these systems exhibit very low critical temperatures when measured in units of the depth of the attractive well, so that any study of their phase transitions requires an accurate description of their properties down to very low temperatures, i.e., in regimes where all the main statistical mechanical tools – computer simulations, integral equations, and perturbation theories – encounter some difficulties.

The present paper stems from two important studies on fluids with very short-ranged interparticle attractions, published thirteen years ago by Vliegenthart and Lekkerkerker (VL)[7] and by Noro and Frenkel (NF),[8] respectively.

The main finding that VL obtained, from computer simulations for a variety of potentials, is the following: as the range of attraction narrows, the critical temperature T_c drops

a)Electronic mail: gazzillo@unive.it
b)Electronic mail: davide.pini@fisica.unimi.it

considerably, but the second virial coefficient

$$B_2(T) = -2\pi \int_0^\infty dr\, r^2\, f(r), \tag{1}$$

when evaluated at the critical temperature, i.e., at $T = T_c$, remains practically constant[7] (here, $f(r) = \exp[-\beta\phi(r)] - 1$ denotes the Mayer function, $\phi(r)$ is the potential, $\beta = (k_B T)^{-1}$ is the inverse temperature, and k_B is the Boltzmann constant). Working with the "reduced" second virial coefficient

$$B_2^* \equiv B_2/B_2^{HS}, \tag{2}$$

where $B_2^{HS} \equiv (2\pi/3)\sigma^3$ refers to hard spheres (HS) with diameter σ, the VL result can be expressed, more precisely, as

$$B_2^{*c} \equiv B_2^*(T_c) \simeq -1.5 \tag{3}$$

(remember that a positive (negative) B_2 means that repulsions (attractions) are predominant). As a consequence, VL proposed the following *empirical criterion for predicting the critical temperature: whenever the reduced second virial coefficient is about* -1.5, *the fluid must be close to its critical temperature.*[7]

To emphasize the importance of B_2, VL recalled that even the conditions for optimum crystallization of a number of globular proteins are characterized by values of the osmotic second virial coefficient, which fall into a narrow interval, the so-called *crystallization slot*.[9] The B_2^* values for optimum crystal growth are however different for different proteins and vary between -1 and -10 .

The NF work shares the opinion that, when the intermolecular potentials $\phi(r)$ have – in addition to a repulsive core – a very short-ranged attractive tail $\phi_{tail}(r)$, the details of this latter part of the interaction are not important. The essential features are only the strength and the effective range of the attractive term. Consequently, one can expect different fluids (within an appropriate class) to exhibit an essentially similar, more or less "universal," behavior.

Noro and Frenkel characterized any physical model with short-ranged interactions by means of only three *scaling parameters*, computed from the knowledge of the interparticle potential alone, without any need for experimental measurements.[8] These parameters are: (1) an "effective" hard core diameter σ_{eff}; (2) an energy scale $\varepsilon = -|\varepsilon|$, which expresses the *strength* of attraction, being equal to the well depth of the attractive tail in the potential; and, finally, (3) the reduced second virial coefficient B_2^*, which allows to quantify the *range of attraction*. In fact, NF defined the "effective" range of an arbitrary attractive potential to be equal to the (temperature-dependent) well-width Δ_{eq} of an "equivalent" square-well (SW) model, that yields the same B_2^* at the same "reduced" temperature $T^* \equiv k_B T/|\varepsilon|$. Exploiting this NF *mapping onto an equivalent square-well* (SW_{eq}), it turns out that, in general, the boundary between stable and metastable vapor-liquid transitions lies within a narrow band around $\Delta_{eq} \simeq 0.14$, in units of σ (according to other authors, the minimum range of attraction is about 1/6 of the range of repulsion[10]).

Using their scaling parameters, NF then proposed an *extended law of corresponding states*,[8] which can be formulated as follows: for a wide class of systems, *all colloidal or protein suspensions having the same values of "reduced" temperature* T^*, *"reduced" density* $\rho^* \equiv (N/V)\sigma_{eff}^3$ (N particles of diameter σ_{eff} in a volume V), *and "reduced" second virial coefficient* B_2^*, *must obey the same reduced equation of state:* $Z = Z(T^*, \rho^*, B_2^*)$.

More recently, the relationship between critical temperature and second virial coefficient was also investigated by Nezbeda *et al.*[11,12] and by Zhou.[13]

As the VL and NF works, the present paper tries to investigate what occurs to the properties of some typical models for colloidal or protein systems, when the range of attraction in the intermolecular potential narrows strongly. In particular, we focus on the second virial coefficient as a simple but interesting quantity, as VL and NF pointed out.

In principle, computer simulations, integral equations, and perturbative methods are the most important tools provided, for such a study, by the modern statistical mechanics of fluids. Here, we will mainly follow an integral equation approach, adding to the well-known Ornstein-Zernike equation[14] the so-called *Self-Consistent Ornstein-Zernike Approximation*, commonly abbreviated as SCOZA closure.[15,16] The reason for this choice is that, for a variety of models, the SCOZA turns out to yield structural and thermodynamic properties in globally good agreement with computer simulations even near phase transitions and in the critical region.[17,20]

In the light of the relevance of the second virial coefficient for systems with short-ranged attractions, it is natural to ask what the SCOZA result for B_2 is. In the present paper, we answer this question by solving the SCOZA self-consistency equation *analytically* at the lowest order in a density expansion scheme. This zero-order result leads to a *fully general* and *analytic* expression for the SCOZA approximations to both the Mayer function and the corresponding second virial coefficient.

In Sec. II these SCOZA analytic expressions are obtained, and in Sec. III they are applied to two prototype models for fluids with short-ranged attractions, namely, the SW and the HS-attractive Yukawa models. For *any* given potential model, comparison between the values of B_2^{SCOZA} and B_2^{exact}, by varying temperature and range of attraction, can be used as a simple tool to determine, at least to a first approximation, the regimes where the performance of SCOZA can be regarded as satisfactory.

In the second part of this work, i.e., Sec. IV, we discuss, both in the exact case and in the SCOZA, the relationship between the behavior of B_2^* at the critical temperature and the vanishing of T_c^* itself, as the range of attraction tends to zero. After revisiting some known results for the SW potential, we perform a thorough analysis of old and new data for the Yukawa model. Finally, Sec. V is dedicated to some conclusions and perspectives.

II. THE SCOZA INTEGRAL EQUATION

The Ornstein-Zernike (OZ) integral equation for a one-component fluid with spherically symmetric interactions is the following relationship between the total and direct

correlation functions, $h(r)$ and $c(r)$, respectively,[14]

$$h(r) = c(r) + \rho \int d\mathbf{r}'\, h(r')c(|\mathbf{r} - \mathbf{r}'|), \tag{4}$$

where $\rho \equiv N/V$ is the number density, $h(r) \equiv g(r) - 1$, and $g(r)$ is the radial distribution function (RDF). For all potentials with a hard-sphere part, i.e.,

$$\phi(r) = \begin{cases} +\infty & r < \sigma \\ \phi_{\text{tail}}(r) & r \geq \sigma \end{cases}, \tag{5}$$

the RDF function must satisfy the exact core condition $g(r) = 0$ for $r < \sigma$.

To solve the OZ equation it is necessary to add a further, approximate relationship between $h(r)$ and $c(r)$, the so-called "closure." The SCOZA reads[15–17]

$$c(r) = c_{\text{HS}}(r) + K(\beta, \rho)\phi_{\text{tail}}(r) \quad \text{for } r \geq \sigma. \tag{6}$$

Here, $c_{\text{HS}}(r)$ denotes the direct correlation function (DCF) of the corresponding HS fluid, and it is assumed to be known. In principle, several choices are possible for it: the simplest one is the Percus-Yevick approximation, i.e., $c_{\text{HS}}(r) = 0$ for $r \geq \sigma$, but a better representation may be given by either the Verlet-Weis[18] or the Waisman[19] parameterization, both with $c_{\text{HS}}(r) \neq 0$ for $r \geq \sigma$.

The factor $K(\beta, \rho)$ depends on the thermodynamic state. The SCOZA closure stems from the *mean spherical approximation* (MSA), which assumes simply $K(\beta, \rho) = -\beta$. Instead, $K(\beta, \rho)$ of SCOZA is not fixed *a priori*, but is determined through the thermodynamic self-consistency requirement between the compressibility (C) and energy (E) routes to thermodynamics. This condition is provided by the thermodynamic identity

$$\frac{\partial}{\partial \beta}\left(\frac{\partial \beta P}{\partial \rho}\right) = \rho \frac{\partial^2 u}{\partial \rho^2} \tag{7}$$

if the pressure P is evaluated via the compressibility equation

$$\frac{\partial \beta P}{\partial \rho} = 1 - 4\pi\rho \int_0^\infty dr\, r^2 c(r), \tag{8}$$

while the excess internal energy per unit volume, u, is given by the energy equation

$$u \equiv \frac{U^{\text{ex}}}{V} = \rho \frac{U^{\text{ex}}}{N} = 2\pi\rho^2 \int_0^\infty dr\, r^2 g(r)\, \phi(r) \tag{9}$$

(here, "excess" is referred to the ideal gas).

Whereas condition (7) is trivially satisfied by the exact pressure and energy, P^{exact} and u^{exact}, in the SCOZA – which is an approximate theory – one must search for some $K(\beta, \rho)$ (if it exists) able to ensure the required self-consistency. Equation (7) is usually reformulated as a diffusion-like partial differential equation (PDE) for u, which must be solved numerically, after specifying the initial condition at $\beta = 0$ as well as two boundary conditions, at $\rho = 0$ (i.e., $u(\beta, \rho = 0) = 0, \forall \beta$) and at the upper boundary ρ_0 of the density interval.[17,20,21]

The finite-difference algorithm used for the numerical integration of this PDE is rather cumbersome, and a necessary step consists in solving the OZ equation supplemented by the SCOZA closure. Unfortunately, it is a common finding that, if the tail $\phi_{\text{tail}}(r)$ of a hard-core potential is very short-ranged, then the solution of the SCOZA-PDE becomes more and more difficult. In fact, in order to obtain a solution independent of the position of ρ_0, this boundary must be moved to very high values, near the close-packing limit, where the numerical algorithm may even fail to converge.[20,21]

In the present paper we try to get some insight into the SCOZA self-consistency condition from an analytical point of view. Our results will then be applied to two of the most typical examples of short-ranged tail potentials.

To this aim, after expanding P, u, c, and g in powers of the density, we will substitute these series into Eqs. (7)–(9). From Eq. (7), together with

$$\beta P = \rho + B_2\rho^2 + \cdots = \rho + \sum_{m=2}^{\infty} B_m \rho^m,$$

$$u = u_2\rho^2 + \cdots = \sum_{m=2}^{\infty} u_m \rho^m,$$

equating the terms corresponding to the same powers of ρ yields a simple relationship between *virial coefficients* B_m and *energy coefficients* u_m:

$$\frac{\partial B_m}{\partial \beta} = (m-1)\, u_m, \quad m \geq 2. \tag{10}$$

This condition may also be rewritten as

$$B_m - B_m^{\text{HS}} = (m-1) \int_0^\beta u_m\, d\beta', \quad m \geq 2, \tag{11}$$

with B_m^{HS} being the mth virial coefficient of the HS fluid.

On the other hand, if $c(r) = \sum_{m=0}^{\infty} c_m(r)\rho^m$, then Eq. (8) implies that the compressibility virial coefficients $(B_m)_C$ can be calculated from the *DCF coefficients* as

$$(B_m)_C = -4\pi \frac{1}{m} \int_0^\infty dr\, r^2 c_{m-2}(r), \quad m \geq 2, \tag{12}$$

where $c_0(r) = f(r)$ is the Mayer function.

Finally, the energy coefficients – hereafter denoted as $(u_m)_E$ to show explicitly that the energy route is used – can be obtained by the *RDF coefficients*. More conveniently, after introducing the cavity function $y(r)$ through the relation $g(r) = e(r)y(r)$, with $e(r) = 1 + f(r)$, one can write

$$g(r) = [1 + f(r)] \sum_{n=0}^{\infty} y_n(r)\rho^n$$

with $y_0 = 1$, and get

$$(u_m)_E = 2\pi \int_0^\infty dr\, r^2\, [1 + f(r)]\, \phi(r)\, y_{m-2}(r), \quad m \geq 2. \tag{13}$$

Using these expressions for the coefficients $(B_m)_C$ and $(u_m)_E$, we can impose the compressibility-energy self-consistency at each order in density, ρ^m, separately. The resulting B_ms represent the SCOZA common values of the compressibility and energy virial coefficients. We shall call them *compressibility-energy* virial coefficients, writing

$$(B_2)_{C,\,E}^{\text{SCOZA}} \equiv (B_2)_C^{\text{SCOZA}} = (B_2)_E^{\text{SCOZA}}.$$

In the following, we will however restrict our study to the lowest order case, that is $m = 2$.

A. SCOZA self-consistency solved analytically at the B_2-level

From Eqs. (10), (12), and (13), applied to hard-core potentials, one finds when $m = 2$

$$\frac{\partial (B_2)_C}{\partial \beta} = (u_2)_E \,,$$

$$(B_2)_C = B_2^{\rm HS} - 2\pi \int_\sigma^\infty dr\, r^2 f(r), \tag{14}$$

$$(u_2)_E = 2\pi \int_\sigma^\infty dr\, r^2 \left[1 + f(r)\right] \phi_{\rm tail}(r)$$

(recall that $f(r < \sigma) = -1$ for hard-core potentials, and $f(r > \sigma) = \exp[-\beta\phi_{\rm tail}(r)] - 1$).

Let us focus on the consistency at the B_2-level. A first remark is that any closure determines a corresponding approximation to the exact Mayer function $f(r)$. Taking the zero-density limit of the SCOZA closure, i.e., $c(r) = c_{\rm HS}(r) + K(\beta, \rho)\phi_{\rm tail}(r)$ for $r \geq \sigma$, one finds $f(r) = f_{\rm HS}(r) + K(\beta, \rho = 0)\phi_{\rm tail}(r)$ for $r \geq \sigma$. Thus, adding the above-mentioned condition $f(r) = -1$ for $r < \sigma$, we obtain

$$f^{\rm SCOZA}(r) = f_{\rm HS}(r) + K_0\, \phi_{\rm tail}(r)\, \Theta(r - \sigma), \quad \forall r \geq 0. \tag{15}$$

Here, $\Theta = 1 + f_{\rm HS}$ is the Heaviside step function ($\Theta(x < 0) = 0$, $\Theta(x > 0) = 1$), while $K_0 \equiv K(\beta, \rho = 0)$ is the zero-order coefficient in the density expansion of $K(\beta, \rho)$, i.e.,

$$K(\beta, \rho) = K_0(\beta) + K_1(\beta)\rho + K_2(\beta)\rho^2 + \cdots.$$

Replacing $f(r)$ with $f^{\rm SCOZA}(r)$ in both $(B_2)_C$ and $(u_2)_E$ yields

$$\begin{cases} (B_2)_C^{\rm SCOZA} = B_2^{\rm HS} - K_0\, I_1 \\ (u_2)_E^{\rm SCOZA} = I_1 + K_0\, I_2 \end{cases}, \tag{16}$$

where

$$I_n \equiv 2\pi \int_\sigma^\infty dr\, r^2\, [\phi_{\rm tail}(r)]^n \,. \tag{17}$$

Thus, the self-consistency at the B_2-level, $\partial B_2/\partial\beta = u_2$, leads to the following differential equation for $K_0(\beta)$:

$$\partial K_0/\partial\beta + \widehat{\varepsilon} K_0 = -1, \quad \text{where } \widehat{\varepsilon} \equiv I_2/I_1 \tag{18}$$

($\widehat{\varepsilon}$ has dimensions of energy), whose solution is

$$K_0(\beta) = \widehat{\varepsilon}^{\,-1}[\exp(-\beta\,\widehat{\varepsilon}) - 1]. \tag{19}$$

It is worth stressing that such a simple expression is *fully general*, i.e., it can be applied to *any* model within the class of the hard-core potentials. Moreover, it shows that, if $\widehat{\varepsilon}$ is very small, then K_0 practically reduces to the MSA limit, i.e., $K_0 = -\beta$.

In principle, our analysis might be extended to the B_3-level, in order to obtain an expression for $K_1(\beta)$. Such a task goes, however, beyond the scope of the present paper.

Our next step will then be the application of the general expression for $K_0(\beta)$ to two of the simplest models of short-ranged tails in hard-core potentials.

III. APPLICATION TO PROTOTYPE MODELS

We shall take into account the two simplest models able to represent fluids with very short-ranged attractions: the SW interaction and the hard-sphere attractive Yukawa (HSAY, or simply HSY) potential. The SW model has no direct interpretation in terms of specific physical effects, but includes empirically both a repulsive and an attractive term, so that it is able to predict vapor-liquid phase transitions. On the other hand, the attractive and repulsive Yukawa potentials may be related to the screened Coulomb interactions occurring in ionic solutions, and by this reason they have often been employed in models for protein suspensions.[22–24]

Within the framework of the studies on very short-ranged attractions, the SW model was investigated through Monte Carlo (MC) computer simulations by Bolhuis *et al.*,[25] López-Rendón *et al.*,[26] and recently by Largo *et al.*[27] The SCOZA integral equation was applied to the SW potential by Schöll-Paschinger *et al.*[20] as well as by Pini *et al.*[21]

As regards the HSY model, many studies – using mainly MC simulations – focused on the relationship between the phase behavior and the range of the attractive potential.[10,25,28–30] The SCOZA approach was employed by Foffi *et al.*,[31] Orea *et al.*,[32] and by Valadez-Peréz *et al.*[24] The paper by Orea *et al.*[32] has been our main source of both MC and SCOZA numerical data for the HSY model.

For all potentials with a HS-part, like those in Eq. (5), from the "exact" B_2 we can get

$$B_{2,\rm ex}^* = -3 \int_1^\infty dx\, x^2\, f(x), \tag{20}$$

where $x \equiv r/\sigma$ is the dimensionless distance and $B_{2,\rm ex}^* \equiv B_2^* - 1$ is the "excess" second virial coefficient, i.e., the excess part – with respect to the HS value – produced by the tail.

A. Square-well tail

In the square-well model, the attractive tail $\phi_{\rm tail}(r)$ is given by

$$\phi_{\rm tail}^{\rm SW}(r) = \begin{cases} \varepsilon = -|\varepsilon| & \sigma \leq r \leq \lambda\sigma \equiv (1 + \Delta)\,\sigma \\ 0 & r > \lambda\sigma \end{cases}. \tag{21}$$

The "exact" reduced second virial coefficient then reads

$$(B_2^*)^{\rm SW\text{-}exact} = 1 - \left[(1 + \Delta)^3 - 1\right](e^{\beta|\varepsilon|} - 1), \tag{22}$$

where $\beta|\varepsilon| = 1/T^*$.

On the other hand, the SCOZA Eqs. (17)–(19) yield $I_1 = B_2^{\rm HS}(\lambda^3 - 1)\varepsilon$, $I_2 = B_2^{\rm HS}(\lambda^3 - 1)\varepsilon^2$, and thus $\widehat{\varepsilon} = \varepsilon$,

$$K_0(\beta) = -|\varepsilon|^{-1}\,(e^{\beta|\varepsilon|} - 1). \tag{23}$$

Equations (15), (16), (21), and (23) then lead to the following important results:

$$f^{\rm SW\text{-}SCOZA}(r) = f^{\rm SW\text{-}exact}(r), \tag{24}$$

$$(B_2)_{C,\,E}^{\rm SW\text{-}SCOZA} = B_2^{\rm SW\text{-}exact}. \tag{25}$$

In brief, for SW potentials, the SCOZA Mayer function always coincides with the exact one, and thus generates – for any *generic* temperature T^* – the fully correct analytic

expression for the compressibility-energy second virial coefficient. The same conclusion can be drawn in the case of a square-shoulder, or square-mound, tail.

B. Attractive Yukawa tail

The Yukawa tail is defined by

$$\phi_{\rm tail}^{\rm HSY}(r) = \varepsilon\,\sigma\,\exp[-z(r-\sigma)]/r, \qquad r \geq \sigma, \tag{26}$$

and is attractive when $\varepsilon = -|\varepsilon|$. The parameter z is related to the range of the Yukawa tail, which can be defined – in dimensionless form – as

$$\Delta_{\rm Y} \equiv (z^*)^{-1}, \quad \text{where } z^* \equiv z\sigma. \tag{27}$$

For the HSAY model, the exact Mayer function and exact B_2 are given, respectively, by

$$f^{\text{HSY-exact}}(x) = \exp\left(\frac{1}{T^*}\frac{e^{-(x-1)/\Delta_{\rm Y}}}{x}\right) - 1, \quad \text{for } x \geq 1, \tag{28}$$

$$(B_2^*)^{\text{HSY-exact}} = 1 - 3\int_1^\infty dx\, x^2\, f^{\text{HSY-exact}}(x). \tag{29}$$

On the other hand, applying our SCOZA formulas leads to $I_1 = 3B_2^{\rm HS}\ \Delta_{\rm Y}(1+\Delta_{\rm Y})\varepsilon$, $I_2 = \frac{3}{2}B_2^{\rm HS}\ \Delta_{\rm Y}\varepsilon^2$, and thus $\widehat{\varepsilon} = \varepsilon/[2(1+\Delta_{\rm Y})]$

$$K_0(\beta) = 2(1+\Delta_{\rm Y})\ \frac{1}{\varepsilon}\left[\exp\left(-\frac{\beta\varepsilon}{2(1+\Delta_{\rm Y})}\right) - 1\right]. \tag{30}$$

Consequently, in the attractive case the SCOZA approximation to the Mayer function is

$$f^{\text{HSY-SCOZA}}(x) = 2(1+\Delta_{\rm Y})\left[\exp\left(\frac{1}{T^*}\,\frac{1}{2(1+\Delta_{\rm Y})}\right) - 1\right] \times \frac{e^{-(x-1)/\Delta_{\rm Y}}}{x} \tag{31}$$

for $x \geq 1$, while the SCOZA B_2 turns out to be

$$(B_2^*)_{C,\,E}^{\text{HSY-SCOZA}} = 1 - 6\Delta_{\rm Y}(1+\Delta_{\rm Y})^2 \times\left[\exp\left(\frac{1}{T^*}\,\frac{1}{2(1+\Delta_{\rm Y})}\right) - 1\right]. \tag{32}$$

This novel analytic expression represents one of the main results of the present paper.

First of all, we can observe that, if the tail range vanishes ($\Delta_{\rm Y} \to 0$) *at constant reduced temperature* T^* – this condition of moving *along a reduced isotherm* must be emphasized – then both $B_2^{\text{HSY-exact}}$ and $B_2^{\text{HSY-SCOZA}}$ tend to $B_2^{\rm HS}$, i.e.,

$$\lim_{\substack{\Delta_{\rm Y}\to 0\\ (T^*=\text{const.})}} (B_2^*)^{\text{HSY-exact}} = \lim_{\substack{\Delta_{\rm Y}\to 0\\ (T^*=\text{const.})}} (B_2^*)_{C,\,E}^{\text{HSY-SCOZA}} = 1. \tag{33}$$

Furthermore, *at fixed* $\Delta_{\rm Y}$, the same HS limit is obtained by taking $T^* \to \infty$, whereas both $B_2^{\text{HSY-exact}}$ and $B_2^{\text{HSY-SCOZA}}$ diverge to $-\infty$ as $T^* \to 0$ (but the former grows faster in absolute value).

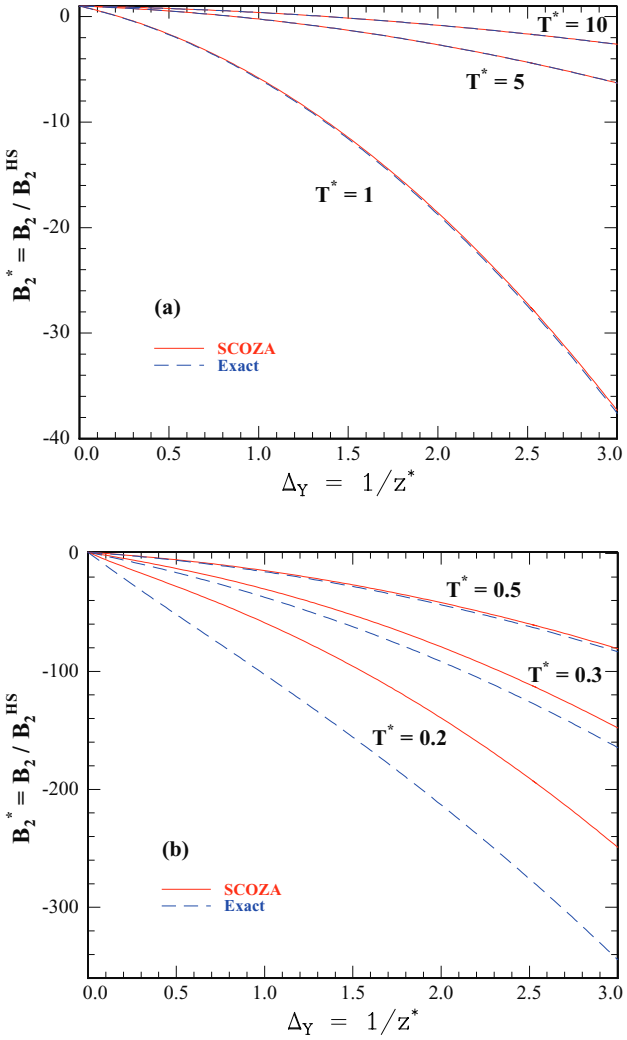

FIG. 1. Reduced second virial coefficient B_2 of the HSY model as a function of the Yukawa range of attraction $\Delta_{\rm Y}$, at several decreasing values of the reduced temperature T^*: (a) High and intermediate temperatures, (b) low temperatures.

From a comparison between $(B_2^*)_{C,\,E}^{\text{HSY-SCOZA}}$ and $(B_2^*)^{\text{HSY-exact}}$ it arises spontaneously a question: how accurate is the SCOZA estimate with respect to the exact result? To test the reliability of SCOZA, we have thus calculated the above-mentioned B_2^*'s as functions of the tail range $\Delta_{\rm Y}$, at several fixed T^*-values. Figure 1 displays our main results.

The agreement of $(B_2^*)_{C,\,E}^{\text{HSY-SCOZA}}$ with $(B_2^*)^{\text{HSY-exact}}$ is excellent at high T^*, over the whole $\Delta_{\rm Y}$-interval considered, and remains good down to $T^* \approx 0.5$. The reason of such a good agreement, at high and intermediate temperatures, can be better understood after expanding these two virial coefficients in powers of $(T^*)^{-1}$, i.e.,

$$(B_2^*)^{\text{HSY-exact}} = 1 - 3\Delta_{\rm Y}(1+\Delta_{\rm Y})\,\frac{1}{T^*} - \frac{3}{4}\Delta_{\rm Y}\frac{1}{T^{*2}} - \frac{1}{2}\int_1^\infty dx\,\frac{e^{-3(x-1)/\Delta_{\rm Y}}}{x}\,\frac{1}{T^{*3}} + \cdots,$$

$$(B_2^*)^{\text{HSY-SCOZA}} = 1 - 3\Delta_Y(1+\Delta_Y)\frac{1}{T^*} - \frac{3}{4}\Delta_Y\frac{1}{T^{*2}} - \frac{1}{8}\frac{\Delta_Y}{1+\Delta_Y}\frac{1}{T^{*3}} + \cdots .$$

The terms up to the second order coincide perfectly. Unfortunately, the satisfactory performance of SCOZA rapidly deteriorates for $T^* \lesssim 0.5$. In any case, the SCOZA values for B_2^* are overestimated with respect to the exact ones: for $\Delta_Y = 1$, the error is about 19% at $T^* = 0.3$ and 43% at $T^* = 0.2$, respectively.

These discrepancies between $B_2^{\text{HSY-SCOZA}}$ and $B_2^{\text{HSY-exact}}$ can be motivated by comparing the corresponding Mayer functions. In Figure 2 we have plotted these f-bonds for decreasing tail ranges ($\Delta_Y = 3, 1, 0.5, 0.1$), at decreasing temperatures ($T^* = 10, 1, 0.5, 0.3$). At low temperatures one finds very large discrepancies, mainly near contact, i.e., at $x \approx 1$–1.5. Here, SCOZA underestimates, in general, the exact f-bonds; as a consequence, $B_2^{\text{HSY-SCOZA}}$ is always less negative than $B_2^{\text{HSY-exact}}$. The differences between the contact values $f^{\text{HSY-exact}}(1^+) = e^{1/T^*} - 1$ and $f^{\text{HSY-SCOZA}}(1^+)$ increase with decreasing T^* and increasing Δ_Y. This behavior is due to the fact that $f^{\text{HSY-exact}}(1^+)$ depends only on T^*, whereas $f^{\text{HSY-SCOZA}}(1^+)$ also changes with varying Δ_Y.

IV. CRITICAL TEMPERATURE AND $B_2(T_c)$

As already mentioned, the second virial coefficient evaluated at the critical temperature, $B_2^{*c} \equiv B_2^*(T_c^*)$, plays an important role in the studies on the phase behavior of colloidal or protein solutions. In particular, it is of special interest to know its dependence on the range of the short-range attractive tail of the potential.

First of all, one must be aware that the limit of $B_2^*(T_c^*)$, as such a tail range vanishes, does not give the HS result. In fact, the HS value comes out when the limit is taken *at constant* T^*, whereas $T_c^* \to 0$, and consequently $1/T_c^* \to +\infty$, if the tail range tends to zero.

A word of caution is, however, necessary. In fact, it is worth stressing that the *vanishing of the tail range* should not be absolutely confused with the so-called *sticky limit* of an attractive interaction. This, really different, idea was originally introduced by Baxter,[33] performing a special limit of a peculiar SW model, whose well becomes infinitesimally narrow, but *simultaneously* infinitely deep, in such a way that

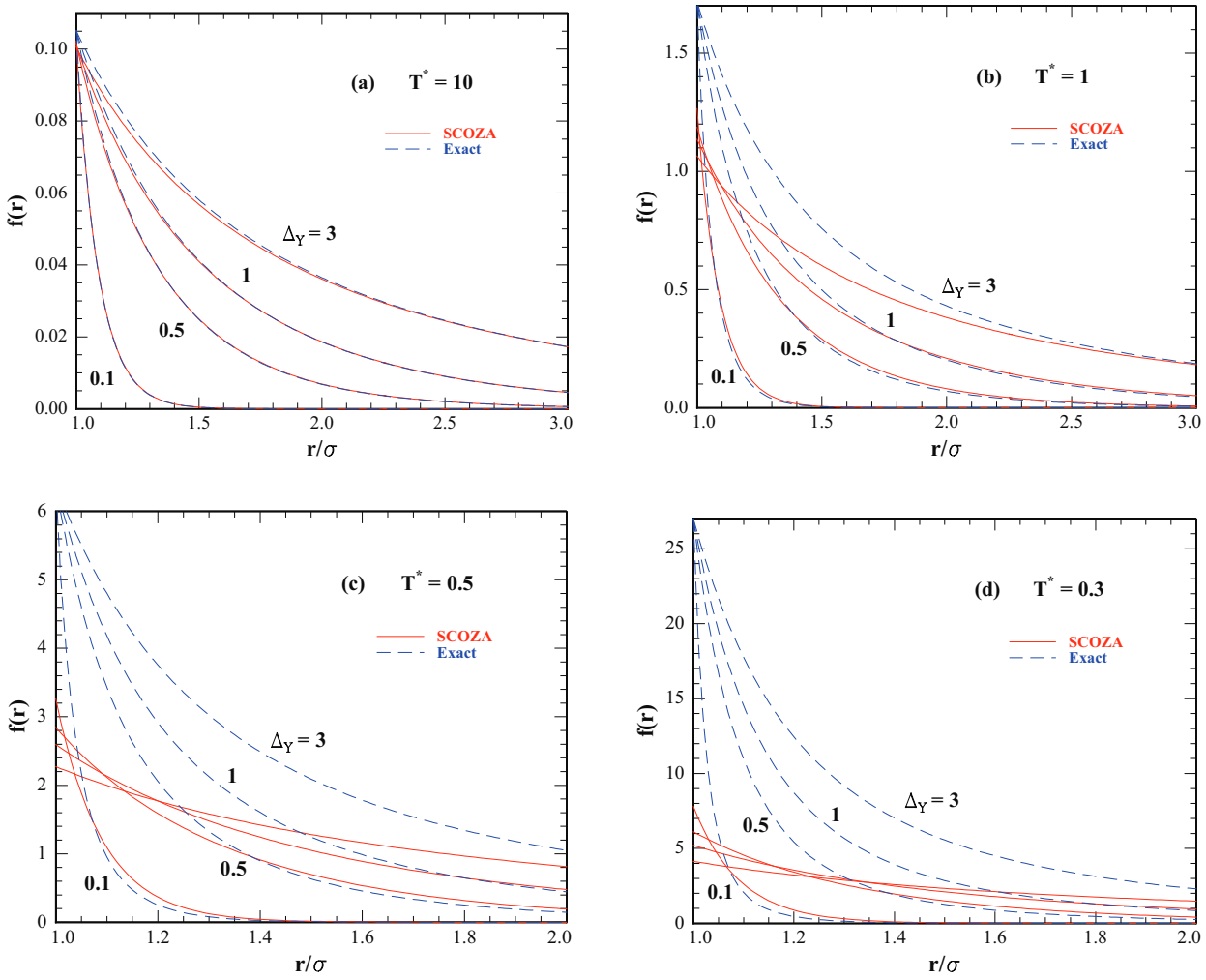

FIG. 2. Comparison between SCOZA and exact Mayer functions for the HSY model, at decreasing reduced temperatures.

the contribution of the attractive tail to B_2^* remains finite and non-zero. More precisely, the starting point is a SW with $|\varepsilon_{\text{Baxter}}| = \beta^{-1}\ln[1 + (12\tau\,\Delta)^{-1}]$, where τ is a Baxter parameter related to stickiness and temperature. Putting $|\varepsilon_{\text{Baxter}}|$ into Eq. (22) and taking the limit $\Delta \to 0$ yields the second virial coefficient for a sticky hard-sphere (SHS) fluid, i.e., $(B_2^*)^{\text{SHS}} = 1 - (4\tau)^{-1}$.

On the analogy of the SW case, the sticky limit of the HSY model should consist in putting $|\varepsilon| = |\varepsilon_0|/\Delta_Y$ and taking the limit $\Delta_Y \to 0$. Unfortunately, such a limit of $(B_2^*)^{\text{HSY-exact}}$ turns out to be divergent,[34,35] so that one must conclude that it is really impossible to define in this way the sticky limit of a HS-Yukawa potential. In the past literature some confusion arose about this point, because of the non-divergence of $(B_2^*)^{\text{HSY-MSA}}$.[34,35] The simultaneous occurrence of a divergent $(B_2^*)^{\text{HSY-exact}}$ and a non-divergent $(B_2^*)^{\text{HSY-MSA}}$ is not surprising, but simply a further example of the thermodynamic inconsistency between the MSA closure and the exact theory.

A. SW simulation data revisited

The vanishing limit of the SW model has been thoroughly investigated, by means of MC computer simulations by Largo *et al.*,[27] down to Δ-values as small as 0.005.

We have employed these MC data for $(T_c^*)^{\text{SW}}$ from Table I of Ref. 27 to calculate, through Eq. (22) with $T^* = T_c^*$, the corresponding simulation results for B_2^{*c}. The Δ-dependence of $(B_2^{*c})^{\text{SW-MC}}$ is shown in the upper panel of Figure 3. The lower panel then displays the Δ-dependence of $(T_c^*)^{\text{SW-MC}}$.

The most remarkable finding is that, in the range $0.005 \le \Delta \le 0.1$, B_2^{*c} for the SW model turns out to be a *nearly linear* function of Δ, so that Largo *et al.*[27] represented this subset of data by $B_2^{*c} = -1.174 - 1.774\Delta$. Before that work, López-Rendón *et al.*[26] had already shown that $(B_2^{*c})^{\text{SW-MC}}$, when examined in a wider interval, is neither a constant nor a linear function of Δ.

Most importantly, the MC simulations by Largo *et al.*[27] indicate that $(B_2^{*c})^{\text{SW-MC}}$ tends to a *finite non-zero* limit as $\Delta \to 0$, i.e., $\lim_{\Delta\to 0} B_2^*(T_c^*) = -1.174$, which – as these authors observed – is slightly higher than the value -1.21, estimated by Miller and Frenkel[36] for the SHS model proposed by Baxter.[33]

Now, the critical temperature of the SW model can rigorously be related to B_2^{*c} solving Eq. (22) as

$$\frac{1}{(T_c^*)^{\text{SW}}} = \ln\left[1 - \frac{\left(B_{2,\text{ex}}^{*c}\right)^{\text{SW}}}{3\Delta\left(1 + \Delta + \frac{1}{3}\Delta^2\right)}\right] = \ln\Delta^{-1} + \ln\frac{-\left(B_{2,\text{ex}}^{*c}\right)^{\text{SW}} + 3\Delta\left(1 + \Delta + \frac{1}{3}\Delta^2\right)}{3\left(1 + \Delta + \frac{1}{3}\Delta^2\right)}. \tag{34}$$

Since the aforesaid, accurate, MC simulations clearly suggest the convergence of B_2^{*c} to a finite non-zero limit, the divergence of $1/(T_c^*)^{\text{SW}}$ as $\Delta \to 0$ is fully characterized by the term $\ln\Delta^{-1}$.

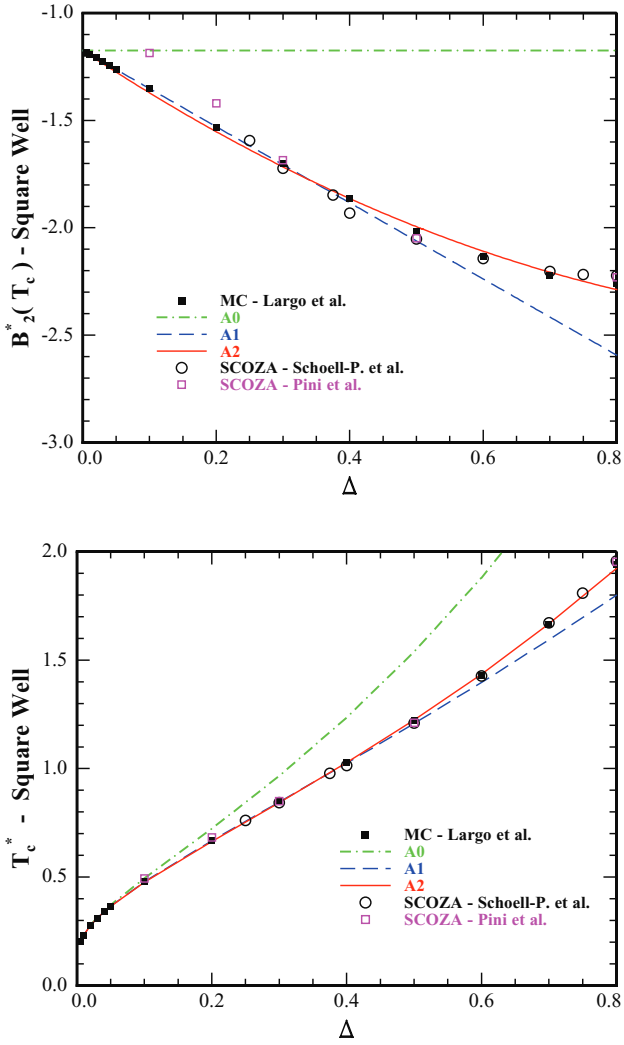

FIG. 3. Upper panel: Three different polynomial approximations to the exact B_2^* of the SW model, as functions of the well-width Δ (filled squares depict the MC simulation data by Largo *et al.*[27]). Lower panel: Three approximations to the SW critical temperature T_c^*, corresponding to the three expressions for B_2^* shown in the upper panel. The SCOZA data are taken from Refs. 20 and 21.

Depending on the approximation chosen for $(B_2^{*c})^{\text{SW}}$ in Eq. (34), we can derive several analytic expressions for $(T_c^*)^{\text{SW}}$ as a function of Δ. The three simplest ones are:

(1) *Zero-order approximation* (A0), which replaces $(B_2^{*c})^{\text{SW}}$ with a *constant* value, as suggested by VL[7] and NF.[8] Largo *et al.*[27] chose

$$B_2^{*c} = B_2^{*c}(\Delta = 0) = -1.174. \tag{35}$$

(2) *First-order approximation* (A1), replacing $(B_2^{*c})^{\text{SW}}$ with the *linear* form

$$(B_2^{*c})^{\text{SW}} = -1.174 - 1.774\Delta, \tag{36}$$

which Largo *et al.*[27] used to fit – over the interval $0.005 \le \Delta \le 0.1$ – their MC data.

(3) *Second-order approximation* (A2). We have fitted all the $(B_2^{*c})^{\text{SW-MC}}$ values – over the whole interval $0.005 \le \Delta$

≤ 0.8 – by the polynomial

$$(B_2^{*c})^{SW} = -1.174 - 2.057\Delta + 0.831\Delta^2. \quad (37)$$

At very small Δ-values, the A0, A1, and A2 predictions for T_c^* are practically indistinguishable, but their differences increase with increasing Δ. The upper panel of Figure 3 shows how the A0 approximation to $(B_2^{*c})^{SW}$ is really crude. Nevertheless, the assumption of constant B_2^{*c} is already sufficient to describe the correct Δ-dependence of T_c^* for small Δ-values, with an error less than 1% up to $\Delta \approx 0.05$ (see the lower panel of Figure 3).

The relative insensitivity of T_c^* to the precise functional form of B_2^{*c}, at least at very small Δ-values, is essentially due to the strong nonlinearity – near the origin – of the logarithmic relationship given by Eq. (34). On the other hand, from a global point of view, it is apparent that A1 improves on A0, while the A2 results are the best ones.

Our conclusions about these approximations are: (1) for the SW model, the constant B_2^{*c} approximation is really acceptable only when working with very short-ranged tails; and (2) a second-order approximation to $B_2^{*c}(\Delta)$ is necessary if one wishes a really good representation of $(T_c^*)^{SW\text{-}MC}$, i.e.,

$$\frac{1}{(T_c^*)^{SW\text{-}MC}} = \ln\left[1 + \frac{0.7247 + 0.686\Delta - 0.277\Delta^2}{\Delta(1 + \Delta + \frac{1}{3}\Delta^2)}\right]. \quad (38)$$

This analytic expression for the SW model may be regarded as a simple parameterization of the MC simulation data, which is accurate at least up to $\Delta \approx 0.8$.

Before concluding this part, it is worth noting that in Figure 3 we have also included SCOZA results for the SW model, available in the literature. After taking all the $(T_c^*)^{SW\text{-}SCOZA}$ data published by Schöll-Paschinger *et al.*[20] as well as by Pini *et al.*,[21] we have derived the corresponding second virial coefficients $(B_2^{*c})^{SW\text{-}SCOZA}$ by calculating $(B_2^*)^{SW\text{-}exact}$, given by Eq. (22), at $T^* = (T_c^*)^{SW\text{-}SCOZA}$. The lower panel of Figure 3 shows that, while the $(T_c^*)^{SW\text{-}SCOZA}$ values are practically coincident with the $(T_c^*)^{SW\text{-}MC}$ ones for $\Delta \gtrsim 0.3$, they start to deviate (in the sense of an overestimation) with respect to the "exact" MC data when $\Delta < 0.3$. These small differences, scarcely appreciable on the scale of this figure, become exponentially amplified when passing to the second virial coefficients displayed in the upper panel. Unfortunately, no SCOZA results for $\Delta < 0.1$ are available at present. Thus, no clear and definitive conclusion can be drawn on the behavior of $(B_2^{*c})^{SW\text{-}SCOZA}$ as $\Delta \to 0$.[21]

However, Figure 3 helps to understand how, although SCOZA yields the exact analytic expression for the second virial coefficient, i.e., $B_2^{*SW\text{-}SCOZA}(T) = B_2^{*SW\text{-}exact}(T)$, nevertheless its *critical* value is not exact in the regime of very short attraction ranges. In fact, $(B_2^{*c})^{SW\text{-}SCOZA}$ stems from two ingredients, since $(B_2^{*c})^{SW\text{-}SCOZA} \equiv B_2^{*SW\text{-}exact}(T_c^{*SW\text{-}SCOZA})$ [whereas $(B_2^{*c})^{SW\text{-}exact} = B_2^{*SW\text{-}exact}(T_c^{*SW\text{-}MC})$], and we have observed that the accuracy of the SW-SCOZA critical temperature deteriorates when Δ becomes very small. Briefly, the exact and SCOZA critical B_2^*'s of the SW model may differ since they involve the same function, but evaluated at different critical temperatures.

TABLE I. SCOZA critical temperatures and densities of the HSY potential in reduced units for several values of the inverse-range parameter z^*.

z^*	T_c^*	ρ_c^*
30	0.21900	0.613
50	0.17713	0.634
60	0.16424	0.635
80	0.14584	0.629
100	0.13306	0.618
150	0.11286	0.581
200	0.10062	0.546
250	0.09219	0.514
350	0.08102	0.462
500	0.07093	0.407
800	0.05989	0.339
1000	0.05539	0.310

B. T_c^* and B_2^{*c} of the Yukawa model

In order to investigate the relationship between T_c^* and B_2^{*c} for the *attractive*-HSY (HSAY) model, we have first collected many simulation data for the HSY critical temperatures available in the literature, and then calculated the corresponding critical second virial coefficients.

From Table I by Orea *et al.*[32] we have taken both "exact" MC and SCOZA results for T_c^* as a function of Δ_Y. Unfortunately, computer simulation data for HSAY fluids with very short-ranged tails – i.e., $z^* > 7$ or $\Delta_Y < 0.14$ – are quite scarce in the literature. To the set $\{T_c^*\}^{MC}$ reported by Orea *et al.*[32] we have thus added one further value found by Dijkstra[10] for the extreme case of $z^* = 100$ ($\Delta_Y = 0.01$), using MC simulations supplemented by thermodynamic integration. In this way, our set $\{T_c^*\}^{MC}$ includes data ranging from $z^* = 1.8$ up to $z^* = 100$, or, equivalently, $0.01 \leq \Delta_Y \leq 0.56$.

The SCOZA predictions for T_c^* were obtained, of course, through a fully numerical solution of the integral equation. Furthermore, to make up for the lack of data in the region of very small Δ_Y-values, we have generated some new SCOZA data. Using the same numerical machinery employed by one of us (D.P.) in the past,[17,32] we have been able to reach really high z^*-values up to $z^* = 1000$, i.e., $\Delta_Y = 0.001$. The accuracy of the numerical calculations was checked by determining *a posteriori* the pressure P and the chemical potential μ by both the compressibility and the internal energy route, and the differences between the two routes were indeed found to be negligible.

Table I of the present paper reports these new SCOZA results for T_c^* and the corresponding critical densities. Technical details about the numerical solution of the SCOZA integral equation relevant to the high-z^* regime may be found in the above-mentioned papers by Schöll-Paschinger *et al.*[20] and by Pini *et al.*[21]

The set $\{B_2^{*c}\}^{MC}$ has been generated by inserting the $\{T_c^*\}^{MC}$ data into Eqs. (28) and (29), and performing the required integration numerically. On the other hand, the set $\{B_2^{*c}\}^{SCOZA}$ has been obtained from $\{T_c^*\}^{SCOZA}$ through the *analytic* expression, Eq. (32). All these T_c^* and B_2^{*c} values are displayed in Figure 4.

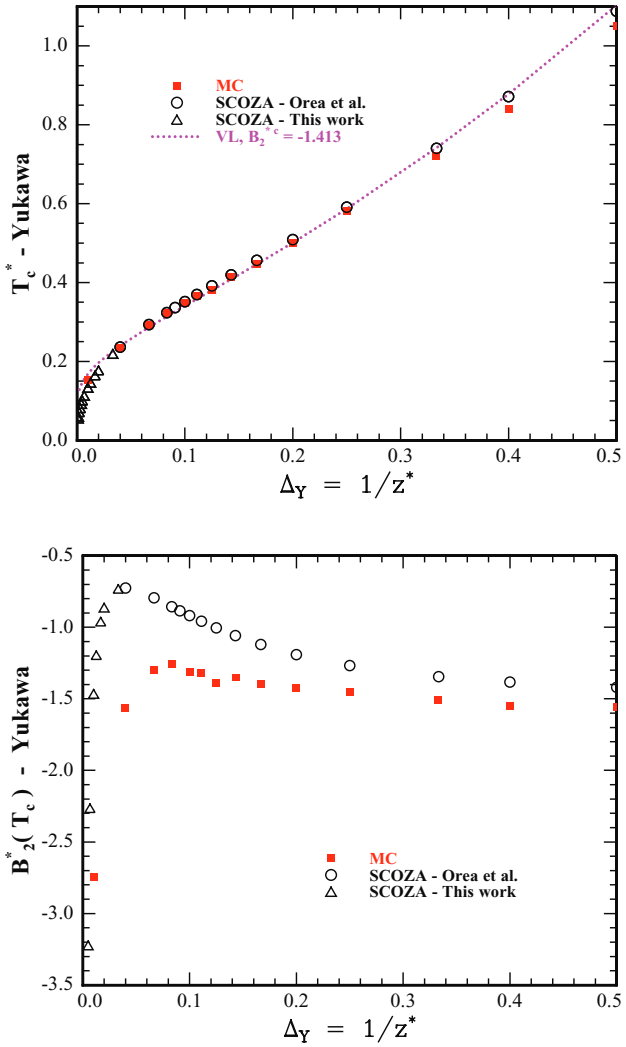

FIG. 4. Comparison between SCOZA and exact MC results for both the critical temperature (upper panel) and the critical second virial coefficient (lower panel), as functions of the attraction range Δ_Y, for the HSY model. In the upper panel, the first two MC points are due to Dijkstra,[10] while the dotted line corresponds to the critical temperatures predicted by the Vliegenthart-Lekkerkerker criterion, as described in the text.

The plot for T_c^* – similar to those shown by Orea *et al.*[32] as well as by Valadez-Pérez *et al.*[24] – looks qualitatively similar to the SW one shown in Figure 3. The SCOZA predictions for T_c^* are in overall good agreement with the MC values in the Δ_Y-interval considered, in particular, for $\Delta_Y \approx 0.04$–0.3.

For $\Delta_Y \gtrsim 0.1$, one finds $(B_2^{*c})^{\text{HSY-MC}} \approx -1.5$, in agreement with the VL hypothesis. On the other hand, the difference between $(B_2^{*c})^{\text{HSY-SCOZA}}$ and $(B_2^{*c})^{\text{HSY-MC}}$ increases on decreasing Δ_Y. This means that at very small tail ranges – which imply very low critical temperatures – the SCOZA closure is no more reliable, from the quantitative point of view. Nevertheless, from the qualitative point of view, both the MC and the SCOZA results seem to agree in showing that the behavior of $(B_2^{*c})^{\text{HSY}}$ for $\Delta_Y \lesssim 0.05$ is apparently different from that of $(B_2^{*c})^{\text{SW}}$ resulting from the simulations by Largo *et al.*[27] Specifically, unlike the SW case, $(B_2^{*c})^{\text{HSY}}$ is *divergent* as Δ_Y vanishes.

However, it should be pointed out that in the MC case such a conclusion is supported by only the two points at smallest Δ_Y obtained in Ref. 10 through simulations complemented by thermodynamic integration. In the light of the sensitiveness of B_2^{*c} to the precise value of T_c^* at small Δ_Y, the production of further MC data in this region would be highly desirable in order to ascertain this point. On the other hand, in the SCOZA the divergence of B_2^{*c} is unquestionable on the basis of the new data generated by us for the present work.

We would also like to stress that such a divergence is not a byproduct of the different functional form of $(B_2^*)^{\text{HSY-SCOZA}}$ with respect to $(B_2^*)^{\text{HSY-exact}}$. In fact, as observed in Sec. III B, $(B_2^*)^{\text{HSY-SCOZA}}$ actually overestimates $(B_2^*)^{\text{HSY-exact}}$. Therefore, for $\Delta_Y \to 0$ a divergence to $-\infty$ is found also if $(B_2^*)^{\text{HSY-exact}}$ is evaluated at the SCOZA critical temperatures $(T_c^*)^{\text{HSY-SCOZA}}$.

C. Test of the VL criterion for predicting $(T_c^*)^{\text{HSY}}$

As mentioned in the Introduction, Vliegenthart and Lekkerkerker[7] asserted that, in general, T_c^* is much less sensitive to the precise form of B_2^{*c} than vice versa. Hence, for the determination of T_c^* it is not necessary to know the second virial coefficient with a great accuracy, but even the approximation of constant B_2^{*c} may be sufficient. Specifically, these authors assumed that the second virial coefficient of colloidal or protein suspensions, at the critical temperature, has the value $(B_2^{*c})_0 \simeq -1.5$. Consequently, we can predict the critical temperature of the HSY model with a given Δ_Y by solving, with respect to T_c^*, the equation

$$[B_2^*(T_c^*, \Delta_Y)]^{\text{HSY-exact}} = (B_2^{*c})_0. \tag{39}$$

Here, one must use the "exact" B_2^*, given by Eqs. (28) and (29). Since this B_2^{*c} is related to T_c^* through the integral of Eq. (29), Eq. (39) can be solved only numerically. It is, however, worth stressing that solving this VL equation is – at this point – a procedure fully independent of the Noro-Frenkel mapping onto an equivalent SW model, which will be discussed later.

Clearly, the divergence of $(B_2^{*c})^{\text{HSY}}$ at the origin strongly contrasts with the VL hypothesis of constant B_2^{*c}. Nevertheless, we have equally applied the VL criterion to the HSY model, after neglecting the diverging portion of the B_2^{*c}-curve.

Instead of the VL value -1.5, in Eq. (39) we have employed our own estimate for $(B_2^{*c})_0$. Indeed, we have determined this constant by fitting the MC data for $(B_2^{*c})^{\text{HSY}}$ displayed in Figure 4 (lower panel), after neglecting the portion of the curve diverging at the origin (in practice, only the first two or three points). From the fit over the interval $0.07 \lesssim \Delta_Y \lesssim 0.56$ we have found the following *zero-order approximation* (B0):

$$(B_2^{*c})^{\text{HSY-MC}} \simeq (B_2^{*c})_0 = -1.413, \tag{40}$$

which lies however close to the VL estimate. Substituting this value into the VL equation (39), and solving it numerically, we have obtained the results displayed as a dotted line in the upper panel of Figure 4.

The agreement between our VL results and the MC data for $(T_c^*)^{\text{HSY}}$ is quite satisfactory for $0.04 \lesssim \Delta_Y \lesssim 0.25$, while

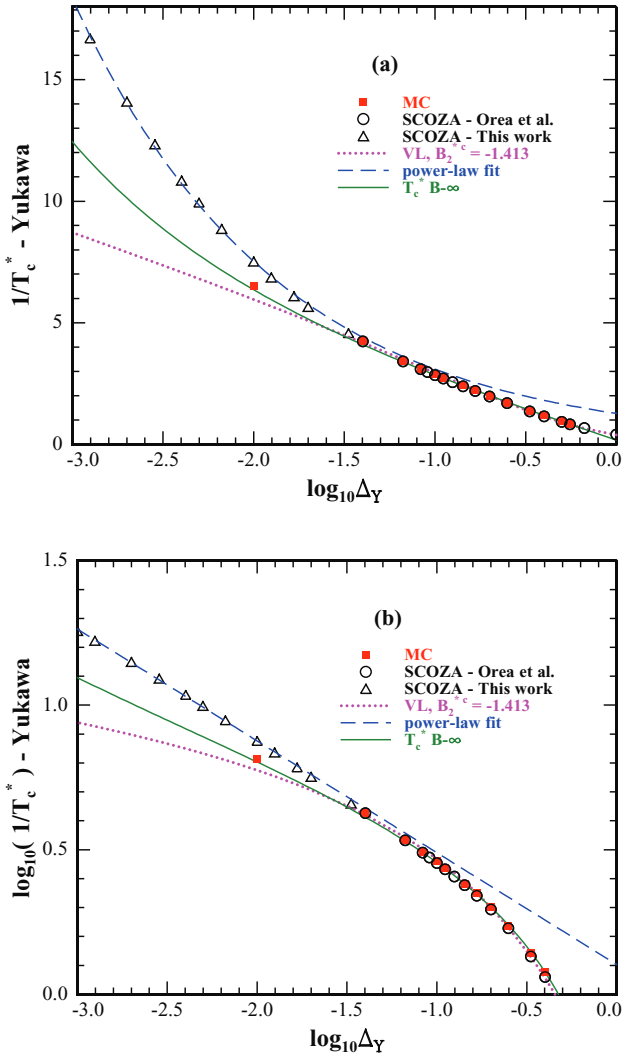

FIG. 5. (a) Symbols depict MC and SCOZA results for the inverse critical temperature of the HSY model, plotted as functions of $\log_{10}\Delta_Y$. Dotted line: predictions obtained by the VL criterion, as in Figure 4. Dashed line: power-law fit, as described in the text. Solid line: analytic representation corresponding to Eq. (43). (b) MC and SCOZA results for the logarithm of the inverse critical temperature, as functions of $\log_{10}\Delta_Y$. Symbols and lines have the same meaning as in (a).

for larger Δ_Y-values our VL curve overestimates the MC results (again as in the SW case), and for very small Δ_Y it is difficult, on the scale of this figure, to assess possible quantitative discrepancies, which will be visualized more clearly in Figure 5. On the other hand, we have verified that using the original VL assumption $B_2^{*c} = -1.5$ would lead to a T_c^*-curve falling only slightly below our VL line. As a consequence, one would get a small improvement for $\Delta_Y \gtrsim 0.3$, but at lower Δ_Y-values the VL curve with $B_2^{*c} = -1.413$ exhibits a slightly better agreement with the MC data.

D. An explicit analytic representation for $(T_c^*)^{HSY}$

Unfortunately, our VL results are merely numerical, while it would be desirable to get some analytic representation of both the critical temperature and the critical second virial coefficient of the HSY model.

Recalling that in the SW model B_2^{*c} does not diverge, while $1/T_c^*$ diverges as $\ln \Delta^{-1}$ when $\Delta \to 0$, one may also wonder how the divergent behavior of $(B_2^{*c})^{HSY}$ depends on that of $(1/T_c^*)^{HSY}$, or vice versa.

In the HSY-SCOZA case, we can take advantage of our analytical expression for $(B_2^{*c})^{HSY\text{-}SCOZA}$, i.e., Eq. (32) together with Eq. (31), which can be rewritten as

$$(B_2^{*c})^{HSY\text{-}SCOZA} = 1 - 3\Delta_Y(1+\Delta_Y)\; f^{HSY\text{-}SCOZA}(1^+; T_c^*), \tag{41}$$

or solved with respect to the critical temperature as

$$\frac{1}{(T_c^*)^{HSY\text{-}SCOZA}} = \ln\left[1 - \frac{\left(B_{2,ex}^{*c}\right)^{HSY\text{-}SCOZA}}{6\Delta_Y(1+\Delta_Y)^2}\right]^{2(1+\Delta_Y)}. \tag{42}$$

Note that the latter expression resembles the SW one, Eq. (34).

Both the exact and the SCOZA B_2^{*c} are related to the Mayer function at the critical temperature. In general, we can state that the behavior of B_2^{*c} depends on the *rate of divergence* of $1/T_c^*$ or, equivalently, of $f(1^+; T_c^*)$.

Hence, to get more insight into the behavior of the HSY model, we have first plotted both the exact and the SCOZA data for $(1/T_c^*)^{HSY}$ as functions of $\ln \Delta_Y$ (see Figure 5(a), where we have used $\log_{10}\Delta_Y$ for a better readability). Then, in Figure 5(b), we have also displayed $\ln(1/T_c^*)^{HSY}$ as a function of $\ln \Delta_Y$ (again replacing ln with $\log_{10}$). A linear portion in Figure 5(a) means a logarithmic dependence – like $\ln \Delta_Y^{-\alpha_1}$ (*weak* divergence; $\alpha_1 > 0$) – in the relevant subinterval, while a linear part in Figure 5(b) highlights a power-law behavior – like $\Delta_Y^{-\alpha_2}$ (*strong* divergence; $\alpha_2 > 0$).

In the right half of Figure 5(a) – which corresponds to $\Delta_Y \gtrsim 0.04$ – both the MC and the SCOZA results for T_c^* agree well with the prediction from the VL hypothesis of a constant B_2^{*c}. Moreover, in this region one also observes that $1/T_c^*$ is really a nearly linear function of $\log_{10}\Delta_Y$. This means that in this subinterval the MC, the SCOZA, and even the VL results, can all be represented by a logarithmic-law. On the contrary, in the left half of Figure 5(a), $1/(T_c^*)^{HSY\text{-}SCOZA}$ deviates significantly from the VL prediction. At the same time, these SCOZA results at very small Δ_Y fall neatly on a straight line when plotted on a $\log_{10}$-$\log_{10}$ scale (see Figure 5(b)). A linear regression, taking into account only the first ten points, gives the following "power-law fit": $1/(T_c^*)^{HSY\text{-}SCOZA} \simeq A\ \Delta_Y^{-\alpha_2}$ with $A \simeq 1.267$ and $\alpha_2 \simeq 0.387$. Clearly, such a power-law divergence of $1/T_c^*$ is too strong to give a finite B_2^{*c} for $\Delta_Y \to 0$, leading instead to the divergence shown in Figure 4. All this means that, at least in the SCOZA case, there exists a crossover between a logarithmic-law behavior for $\Delta_Y \gtrsim 0.04$ and a power-law behavior for $\Delta_Y \lesssim 0.04$.

In the small-Δ_Y regime, a deviation from the VL prediction is observed also for the MC results, as expected on the basis of the behavior of $(B_2^{*c})^{HSY\text{-}MC}$ discussed above. However, the extent of the deviation is smaller than that found in SCOZA, and the paucity of MC data in this region does not allow one to obtain any reliable indication on the dependence

of $1/(T_c^*)^{\text{HSY-MC}}$ on Δ_Y in the region closest to the origin. Nevertheless, it may be useful to provide a simple analytical parameterization of all the available MC results over the interval $0 \le \Delta_Y \lesssim 0.5$. To this purpose, we have empirically fitted $1/(T_c^*)^{\text{HSY-MC}}$ by means of the sum of a logarithmic and a power-law term, according to the following expression:

$$\frac{1}{(T_c^*)^{\text{HSY-B-}\infty}} \simeq \ln \Delta_Y^{-1} + \frac{0.175}{\Delta_Y^{1/2}}. \tag{43}$$

As shown in Figure 5, this very simple form does give an accurate representation of $1/(T_c^*)^{\text{HSY-MC}}$, at least within the interval considered here. A word of caution may, however, be appropriate: we do not claim that the exponent 1/2 in the power term is the "exact" one. It should be regarded only as a good guess, leading to an accurate description of the MC results available at present, but having no special physical meaning. Consequently, it should not be taken too literally, since a close value might be equally well acceptable.

E. $(B_2^{*c})^{\text{HSY-MC}}$ and the NF mapping onto an equivalent SW

A simple analytic representation for $(B_2^{*c})^{\text{HSY-MC}}$ is more difficult to obtain, since the exact relationship between B_2^{*c} and $1/T_c^*$ involves an integral. In order to bypass such a numerical problem and get an analytic approximation for $(B_2^{*c})^{\text{HSY-MC}}$, we can resort to the Noro-Frenkel suggestion of mapping the attractive-HSY potential onto an equivalent SW_{eq} model.[8] The NF recipe allows to write, at any temperature T^*,

$$(B_2^*)^{\text{HSY}} = (B_2^*)^{\text{SW}_{\text{eq}}} = 1 - D^{\text{HSY}}(T^*)(e^{1/T^*} - 1), \tag{44}$$

with

$$D^{\text{HSY}}(T^*) \equiv [1 + \Delta_{\text{HSY,eq}}(T^*)]^3 - 1, \tag{45}$$

where $\Delta_{\text{HSY, eq}}(T^*)$ is the width of the well equivalent to the HSY tail.

At the critical temperature, we have computed directly $D(T_c^*) = -B_{2,\text{ex}}^{*c}/(e^{1/T_c^*} - 1)$ from the simulation data for $(T_c^*)^{\text{HSY-MC}}$ and $(B_{2,\text{ex}}^{*c})^{\text{HSY-MC}}$, and fitted this quantity with a simple polynomial, i.e.,

$$D(T_c^*) \simeq \Delta_Y \left(0.857 + 5.393\Delta_Y - 1.346\Delta_Y^2\right), \tag{46}$$

for $0 \le \Delta_Y \lesssim 0.7$.

In passing, note that we do not need the explicit calculation of $\Delta_{\text{HSY,eq}}(T_c^*)$, which may however be obtained – as a byproduct – from $\Delta_{\text{HSY,eq}}(T_c^*) = \sqrt[3]{1 + D^{\text{HSY}}(T_c^*)} - 1$.

From Eqs. (43), (44), and (46), we can now obtain an analytic approximation to $(B_2^{*c})^{\text{HSY-MC}}$, which reads

$$(B_2^{*c})^{\text{HSY, SW}_{\text{eq}}\text{-B-}\infty} = 1 - \left(0.857 + 5.393\Delta_Y - 1.346\Delta_Y^2\right) \times \left[\exp\left(\frac{0.175}{\Delta_Y^{1/2}}\right) - \Delta_Y\right]. \tag{47}$$

The label B-∞ serves to recall that this expression for the second virial coefficient does diverge at the origin (the same label has already been employed in Eq. (43), to stress that it is conjugate to the present one). The corresponding results are shown in Figure 6.

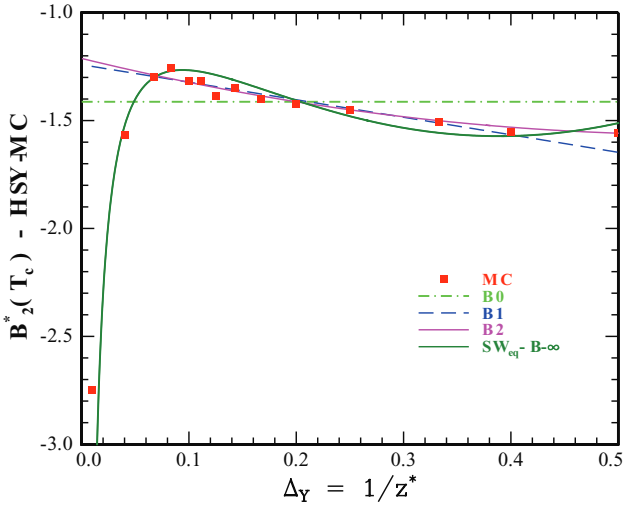

FIG. 6. Several approximations to the exact MC results for B_2^{*c} of the HSY model. The label B-∞ refers to Eq. (47).

Now, we can also complete the discussion of Sec. IV C on the VL criterion for predicting the critical temperature, by exploiting the NF mapping, which allows to write

$$\frac{1}{(T_c^*)^{\text{HSY-SW}_{\text{eq}}}} = \ln\left[1 + \frac{\left(-B_{2,\text{ex}}^{*c}\right)^{\text{HSY-MC}}}{\Delta_Y\left(0.857 + 5.393\Delta_Y - 1.346\Delta_Y^2\right)}\right]. \tag{48}$$

In this equation $1/T_c^*$ is again related to B_2^{*c} through a logarithmic function, so that even a large variation of B_2^{*c} turns out to be practically inconsequential, as affirmed by the VL criterion.

We will indeed study the effect of using different approximations to $(B_2^{*c})^{\text{HSY-MC}}$ – of increasing accuracy – in Eq. (48).

In addition to the *zero-order approximation* (B0) already introduced in Sec. IV C, we take into account two other approximations without the diverging portion of the curve:

(1) *First-order or linear approximation* (B1):

$$(B_2^{*c})^{\text{HSY-MC}} \simeq -1.241 - 0.812\ \Delta_Y. \tag{49}$$

(2) *Second-order approximation* (B2):

$$(B_2^{*c})^{\text{HSY-MC}} \simeq -1.212\ (1 + \Delta_Y) + 1.038\ \Delta_Y^2. \tag{50}$$

All the considered approximations are shown in Figure 6.

As B0-, the B2-expression has been obtained by fitting over the interval $0.07 \lesssim \Delta_Y \lesssim 0.56$, whereas the B1-one refers to the more restricted, nearly linear, portion $0.07 \lesssim \Delta_Y \le 0.4$.

The values of T_c^* predicted by all these approximations to B_2^{*c} – through the SW_{eq} mapping – are finally plotted in Figure 7 (for comparison, we have also plotted the expression given by Eq. (43), with the same label B-∞ used for its

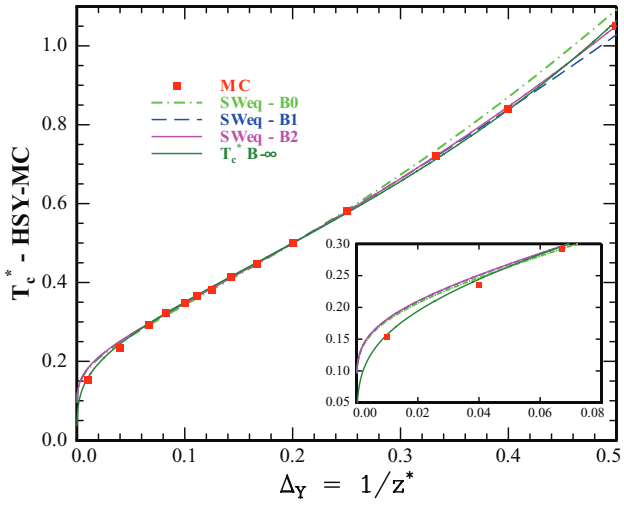

FIG. 7. Comparison among several predictions for T_c^* of the HSY model, corresponding to the approximations to B_2^{*c} shown in Figure 6. The solid line with label B-∞ corresponds to Eq. (43). The inset magnifies the portion closest to the origin.

conjugate second virial coefficient). Although the crude constant-B_2^{*c} approximation yields results which are good enough, in the region (0.25, 0.5) the B1- and B2-expressions do provide a progressively better agreement with the MC data.

However, a merely visual judgement cannot be fully reliable. Rigorously speaking, the predictions by all these formulas with a non-diverging second virial coefficient correspond to a behavior near the origin different from that described by Eq. (43). Indeed, B0, B1, and B2 all imply a *weak* divergence of $(1/T_c^*)^{\mathrm{HSY}}$, since in these cases Eq. (48) produces only a divergent term $\ln \Delta_Y^{-1}$, exactly as in the SW model. These differences become, however, really significant only for $0 \le \Delta_Y \lesssim 0.04$, as can be appreciated from the inset of Figure 7, where the portions nearest to the origin of all these T_c^*-curves are magnified.

It is again worth emphasizing that our interest in the region of very short ranges of attraction, extending down to the origin, is an important characteristic of the present study. All our figures displaying directly the critical temperatures, both for the SW and HSY models (namely, Figs. 3, 4, and 7), illustrate the behavior of T_c^* even when the range of attraction vanishes. Furthermore, we have discussed the problem of the rate of vanishing of T_c^*, which has an influence on how the critical second virial coefficient depends on the range of attraction near the origin. A comparison can be made, for instance, with Figs. 14 and 15 by Valadez-Pérez *et al.*,[24] which show the critical temperatures of the HCAY, Asakura-Oosawa, and SW models as functions of the interaction range (or the "effective" interaction range λ). These figures are very similar to ours, but are restricted to the nearly linear portion of the T_c^*-curves, omitting completely the origin. In particular, Fig. 14 refers to the interval $0.05 \le \Delta_Y \le 0.35$, and Valadez-Pérez *et al.*[24] fitted the corresponding simulation data for the HCAY fluid with a linear function $(T_c^*)^{\mathrm{HSY\text{-}MC}} = 0.190(5) + 1.586(26)\Delta_Y$ (similar linear functions were also proposed by these authors for other potential models). Unfortunately, this range-dependence law cannot be extrapolated down to the origin, since it is evident that such linear functions cannot satisfy the physically based boundary condition that, in general, the critical temperature of any fluid must vanish when the attractions tend to zero.[10]

Although this paper is mostly concerned with the behavior of T_c^* and B_2^{*c}, it is worthwhile concluding this section by observing that the deviations of SCOZA from the VL-NF predictions as $\Delta_Y \to 0$ involve also the critical density ρ_c^*. In fact, on the basis of the NF generalized law of corresponding states, one expects that, in this limit, ρ_c^* of the HCY fluid should tend to a limit close to the value $\rho_c^* = 0.552$ obtained by the accurate MC simulations of Largo *et al.*[27] for a SW potential of vanishing width. However, inspection of Table I shows that for $\Delta_Y \to 0$ the SCOZA ρ_c^* does not appear to saturate to a finite value, but rather follows a non-monotonic behavior: on decreasing Δ_Y, it increases at first, but takes a maximum $\rho_c^* \simeq 0.635$ for $1/\Delta_Y \simeq 60$, and then decreases as Δ_Y is further decreased. Unfortunately, the MC simulations for small Δ_Y of Ref. 10 do not report results for ρ_c^*, so we are not in a position to make any comparison with other simulations in this regime.

V. CONCLUSIONS

The present work has focused on the possibility of an accurate statistical mechanical description of fluids even when the attractive part of their intermolecular potentials, which may include a hard-sphere term, turns out to be *extremely short-ranged*. This situation, very common for colloidal suspensions or protein solutions, represents a really hard problem for all the most employed approaches of the statistical mechanical theory, i.e., integral equations – and specifically the OZ equation with the SCOZA closure – as well as MC simulations, or perturbation theories. Thus, any progress about the applicability of these methods to such demanding regimes can also contribute, in principle, to a better understanding of experimental data relevant to colloidal/protein physical systems.

Let us summarize the main results of the paper.

(1) We have determined the general analytic expression of $K_0(\beta)$, the zero-order term in the density expansion of $K(\beta, \rho)$, the state-dependent parameter which ensures, in the SCOZA closure, the self-consistency between compressibility and energy routes to thermodynamics. Our result can be applied to *any* HS potential with a tail, and allows to derive analytically the corresponding SCOZA approximation to the Mayer function and thus to the second virial coefficient.

(2) It has been demonstrated that, for SW as well as square-shoulder fluids, the SCOZA second virial coefficient always has the *exact* analytic form, while this is not the case for a generic tail potential. However, the equality $B_2^{*\mathrm{SW\text{-}SCOZA}} = B_2^{*\mathrm{SW\text{-}exact}}$ at a generic temperature T^* does not imply that the critical SCOZA second virial coefficient $(B_2^{*c})^{\mathrm{SW\text{-}SCOZA}}$ is always exact. In fact, this quantity is obtained by evaluating $B_2^{*\mathrm{SW\text{-}exact}}$ at the SCOZA critical temperature $(T_c^*)^{\mathrm{SW\text{-}SCOZA}}$, which deviates from the "exact" MC one when Δ becomes very small.

(3) The analytic formula for B_2^{SCOZA} may help to estimate the reliability of SCOZA for a given model in a given

regime: when the values of $B_2^{\mathrm{SCOZA}}(T^*)$ and $B_2^{\mathrm{exact}}(T^*)$ – evaluated *at the same temperature* (as in all cases illustrated by Figure 1, which refers to the HSY model for several values of T^*) – begin to differ significantly, then the SCOZA closure is breaking down. Clearly, such a criterion does not apply to the SW potential, since in this peculiar case the equality $B_2^{\mathrm{SCOZA}}(T^*) = B_2^{\mathrm{exact}}(T^*)$ is identically satisfied. This fact might suggest that SCOZA should work perfectly for the SW model, whereas it is known[20,21] that SCOZA deteriorates for very short-ranged SW fluids, and seems to perform better for the HSY case, although the analytic expressions of $B_2^{\mathrm{HSY\text{-}SCOZA}}$ and $B_2^{\mathrm{HSY\text{-}exact}}$ are different. Perhaps, to explain this counter-intuitive behavior, one might guess a compensation of errors in the SCOZA virial expansion. Unfortunately, a discussion on this point would require the extension of our study to the SCOZA higher-order virial coefficients, i.e., B_m^{SCOZA} with $m > 2$, which is not trivial even for $m = 3$ and goes beyond the scope of the present paper.

(4) A special attention has been paid to the regime of extremely short-ranged attractions (very close to the origin of the Δ- or Δ_{Y}-axis), for both the HSY and SW potentials. We have investigated, as the range of attraction tends to zero, the rate of vanishing of T_{c}^*. To this aim, we have generated, in particular, a new set of SCOZA results for the attractive-HSY model in the region of extremely narrow Yukawa tails.

(5) The HSY second virial coefficient satisfies the Vliegenthart-Lekkerkerker criterion for $\Delta_{\mathrm{Y}} \gtrsim 0.1$, but diverges as the tail range vanishes. The corresponding SCOZA estimate exhibits qualitatively the correct trend, but differs quantitatively from the exact value when Δ_{Y} becomes very small.

(6) From fitting the available MC data, we have empirically found an extremely simple approximation to the critical temperature of the Yukawa model, i.e.,

$$(T_{\mathrm{c}}^*)^{\mathrm{HSY\text{-}MC}} \simeq \frac{\Delta_{\mathrm{Y}}^{1/2}}{0.175 - \Delta_{\mathrm{Y}}^{1/2} \ln \Delta_{\mathrm{Y}}} \tag{51}$$

(previously denoted as $(T_{\mathrm{c}}^*)^{\mathrm{HSY\text{-}B\text{-}\infty}}$), which is accurate within the interval of narrow tails $0 \leq \Delta_{\mathrm{Y}} \lesssim 0.5$. A corresponding analytic expression has also been determined for the second virial coefficient.

(7) For the HSY model, the VL-NF hypothesis of using a constant-B_2 approximation to predict the critical temperature works sufficiently well for $0.04 \lesssim \Delta_{\mathrm{Y}} \lesssim 0.25$. On the contrary, a better, polynomial, approximation to $(B_2^{*\mathrm{c}})^{\mathrm{exact}}$ is required for a really accurate determination of T_{c}^* when $\Delta_{\mathrm{Y}} \gtrsim 0.25$. Furthermore, in the regime of very short-ranged Yukawa tails – corresponding to $\Delta_{\mathrm{Y}} \lesssim 0.04$ – the divergence of B_2 at the origin cannot be neglected.

In future perspective, the present work remains open to possible analytic extensions, which could obtain the expressions for the next, higher-order, SCOZA coefficients, i.e., $K_n(\beta)$ with $n \geq 1$.

One may wonder whether the SCOZA would predict a negatively diverging $B_2^{*\mathrm{c}}$ in the limit of vanishing attraction range also for different tail potentials. Unfortunately, for a generic tail one has to turn to a fully numerical algorithm, whose solution for very narrow interactions poses severe difficulties.[20,21] Nevertheless, it is worthwhile recalling that in Ref. 21 the application of SCOZA to the SHS model was considered. This model, as recalled in Sec. IV, is obtained from a SW potential when the limit of vanishing attraction range and infinite well depth are taken simultaneously, in such a way that B_2 remains finite. Quite unexpectedly, it was found that SCOZA fails to give a critical point and fluid-fluid phase separation for this model. As pointed out above, the SHS model refers to a situation different from the limit of vanishing tail range at constant well depth considered here. Still, this result represents another instance, in which the requirement of the existence of a critical point with a finite B_2 cannot be fulfilled within SCOZA.

As far as the MC results are concerned, the evidence of a diverging B_2 at the critical temperature for $\Delta_{\mathrm{Y}} \to 0$ is admittedly weaker than in SCOZA. In fact, the number of simulation data for very small Δ_{Y} is scarce, with just two cases for $z^* = 1/\Delta_{\mathrm{Y}} \geq 25$ that we are aware of.[10] Moreover, notwithstanding the accuracy of those simulations, one should keep in mind that in this regime of small Δ_{Y} and small T_{c}^*, even a small uncertainty in T_{c}^* entails significant deviations in $B_2^{*\mathrm{c}}$. Hence, we hope that the present paper may stimulate the production of new MC data for the HSY potential in the most demanding regime of extremely short-ranged tails.

Finally, some theoretical work on the exact rate of divergence of $1/T_{\mathrm{c}}^*$ in the HSY model would also be highly desirable.

[1] B. J. Alder and T. E. Wainwright, J. Chem. Phys. **27**, 1208 (1957).
[2] W. W. Wood and J. D. Jacobson, J. Chem. Phys. **27**, 1207 (1957).
[3] V. I. Kalikmanov, *Statistical Physics of Fluids* (Springer, Berlin, 2001).
[4] J. L. Barrat and J. P. Hansen, *Basic Concepts for Simple and Complex Liquids* (Cambridge University Press, Cambridge, 2003).
[5] D. Rosenbaum, P. C. Zamora, and C. F. Zukoski, Phys. Rev. Lett. **76**, 150 (1996).
[6] M. Muschol and F. Rosenberger, J. Chem. Phys. **107**, 1953 (1997).
[7] G. A. Vliegenthart and H. N. W. Lekkerkerker, J. Chem. Phys. **112**, 5364 (2000).
[8] M. G. Noro and D. Frenkel, J. Chem. Phys. **113**, 2941 (2000).
[9] A. George and W. W. Wilson, Acta Crystallogr., Sect. D: Biol. Crystallogr. **50**, 361 (1994).
[10] M. Dijkstra, Phys. Rev. E **66**, 021402 (2002).
[11] I. Nezbeda and W. R. Smith, Fluid Phase Equilib. **216**, 183 (2004).
[12] J. Krejčí and I. Nezbeda, Fluid Phase Equilib. **314**, 156 (2012).
[13] S. Zhou, Mol. Simul. **33**, 1187 (2007).
[14] J. P. Hansen and I. R. McDonald, *Theory of Simple Liquids*, 3rd ed. (Academic, New York, 2006).
[15] J. S. Høye and G. Stell, J. Chem. Phys. **67**, 439 (1977).
[16] J. S. Høye and G. Stell, Mol. Phys. **52**, 1071 (1984).
[17] D. Pini, G. Stell, and N. B. Wilding, Mol. Phys. **95**, 483 (1998).
[18] L. Verlet and J. J. Weis, Phys. Rev. A **5**, 939 (1972).
[19] E. Waisman, Mol. Phys. **25**, 45 (1973).
[20] E. Schöll-Paschinger, A. L. Benavides, and R. Castañeda-Priego, J. Chem. Phys. **123**, 234513 (2005).
[21] D. Pini, A. Parola, J. Colombo, and L. Reatto, Mol. Phys. **109**, 1343 (2011).
[22] J. Li, R. Rajagopalan, and J. Jiang, J. Chem. Phys. **128**, 235104 (2008).
[23] C. Gögelein, D. Wagner, F. Cardinaux, G. Nägele, and S. U. Egelhaaf, J. Chem. Phys. **136**, 015102 (2012).
[24] N. E. Valadez-Pérez, A. L. Benavides, E. Schöll-Paschinger, and R. Castañeda-Priego, J. Chem. Phys. **137**, 084905 (2012).
[25] P. Bolhuis, M. Hagen, and D. Frenkel, Phys. Rev. E **50**, 4880 (1994).
[26] R. López-Rendón, Y. Reyes, and P. Orea, J. Chem. Phys. **125**, 084508 (2006).
[27] J. Largo, M. A. Miller, and F. Sciortino, J. Chem. Phys. **128**, 134513 (2008).
[28] E. Lomba and N. G. Almarza, J. Chem. Phys. **100**, 8367 (1994).

[29]M. H. J. Hagen and D. Frenkel, J. Chem. Phys. **101**, 4093 (1994).
[30]Y. Duda, A. Romero-Martínez, and P. Orea, J. Chem. Phys. **126**, 224510 (2007).
[31]G. Foffi, G. D. McCullagh, A. Lawlor, E. Zaccarelli, K. A. Dawson, F. Sciortino, P. Tartaglia, D. Pini, and G. Stell, Phys. Rev. E **65**, 031407 (2002).
[32]P. Orea, C. Tapia-Medina, D. Pini, and A. Reiner, J. Chem. Phys. **132**, 114108 (2010).
[33]R. J. Baxter, J. Chem. Phys. **49**, 2770 (1968).
[34]D. Gazzillo and A. Giacometti, Mol. Phys. **101**, 2171 (2003).
[35]D. Gazzillo, J. Chem. Phys. **134**, 124504 (2011).
[36]M. A. Miller and D. Frenkel, Phys. Rev. Lett. **90**, 135702 (2003).